Heterogeneous atmospheric degradation of current-use pesticides by nitrate radicals

Coraline Mattei, Henri Wortham, Etienne Quivet

Heterogeneous atmospheric degradation of Current-Use Pesticides by nitrate radicals

Coraline MATTEI [a,b], Henri WORTHAM [a], Etienne QUIVET [a,*]

[a] Aix Marseille Univ, CNRS, LCE, Marseille, France

[b] French Environment and Energy Management Agency 20, avenue du Grésillé, BP 90406, 49004 Angers Cedex 01, France

Submitted to Atmospheric Environment

***Corresponding author:** Phone: +33 413551054; fax: +33 413551060; e-mail address: etienne.quivet@univ-amu.fr

ABSTRACT

In the atmosphere, pesticides are distributed between gaseous and particulate phases according to their physicochemical properties. In these two phases, they can react with atmospheric oxidants such as ozone, hydroxyl radical and nitrate radicals. Heterogeneous kinetics of the degradation by nighttime nitrate radicals are not well described. In this study, the heterogeneous reactivity with nitrate radicals of eight current-use pesticides (i.e., difenoconazole, tetraconazole, cyprodinil, fipronil, oxadiazon, pendimethalin, deltamethrin, and permethrin) adsorbed on silica model particles was investigated using laboratory experiments with in-situ nitrate radicals generation and concentration measurement. Under these experimental conditions, all pesticides were degraded. Atmospheric half-lives calculated with a Langmuir-Rideal model ranged between 8 days and 16 days and between 2 days to 11 days according to a Langmuir-Hinshelwood model for an atmospheric nitrate radicals concentration of 20 ppt. Results obtained can contribute to a better understanding of the atmospheric fate of pesticides in the particulate phase and show the importance of their degradation by nitrate radical compared to their degradation by other oxidants such as ozone and hydroxyl radicals.

GRAPHICAL ABSTRACT

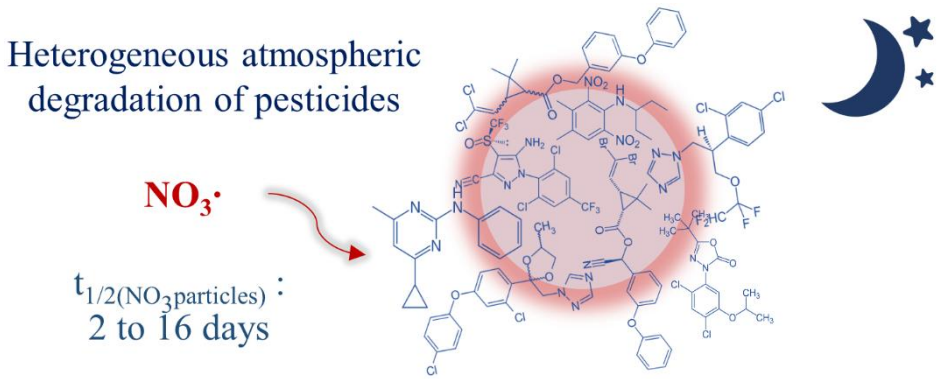

KEYWORDS: pesticides, nitrate radicals, heterogeneous reactivity, kinetics, atmosphere

HIGHLIGHTS:

- Laboratory experiments at an atmospheric relevant concentration of NO_3 radicals
- Current-use pesticide studied were degraded by NO_3 radicals in the particle phase
- Heterogeneous half-lives of pesticides toward NO_3 radicals range from 2 to 16 days
- NO_3 radicals must be considered for the heterogeneous degradation of pesticides

INTRODUCTION

Pesticides are widely used in agriculture and for sanitary purposes. In 2016, they represented a 50 billion dollar annual market worldwide only concerning crop protection (UIPP, 2017). However, because of their environmental and health effects (Inserm, 2013; Carvalho, 2017), they stand for an important topic of interest to both the scientific community and the general public. When applied, up to 40% of pesticides can be lost to the atmosphere (Sinfort et al., 2009; Yates et al., 2015; Zivan et al., 2016,2017). They can be dispersed and transported up to a global scale. As a result, pesticides are found worldwide in the atmosphere, even in Antarctica where no use of them was ever reported (Khairy et al., 2016). In the atmosphere, according to their physicochemical properties, pesticides are partitioned between the aqueous, the gaseous, and the particulate phases, where they can react with atmospheric oxidants. Current-use pesticides are poorly present in the aqueous phase due to their low water solubility. In the gas phase, their atmospheric reactivity has been studied and their rate constant with hydroxyl radicals and, to a lesser extent, with ozone can be estimated

(Atmospheric Oxidation Program for Microsoft Windows, AOPWIN^{TM} Software, (Meylan and Howard, 1993)). As semi-volatile compounds, most of them are partly adsorbed on the surface of atmospheric particles (Sauret et al., 2008) and little is known about their heterogeneous reactivity.

Major atmospheric oxidants are ozone (O_3), hydroxyl radicals (OH), and nitrate radicals (NO_3). Heterogeneous degradation by ozone and OH radicals was already studied for some pesticides (Borrás et al., 2015; Chen et al., 2016; Socorro et al., 2016; Mattei et al., 2018), but their degradation by nitrate radicals is poorly described (Yang et al., 2011; Liu et al., 2011, 2012, 2015; Wang et al., 2012, 2013; Li et al., 2014). Nitrate radicals are present during the night in concentration from a few ppt (Khan et al., 2008; Crowley et al., 2010) up to several hundreds of ppt (Atkinson et al., 1985; Asaf et al., 2010) and could, therefore, have a significant impact on the atmospheric half-life of pesticides.

Previous studies have shown significant reactivity of nitrate radicals with volatile organic compounds in the atmosphere (Ng et al., 2017). In particular, studies show that reactivity of organic compounds with nitrate radicals is generally slower than with hydroxyl radicals. Nevertheless, the more important atmospheric concentrations of NO_3 radicals compared to OH radicals leads to a similar or greater oxidation power of NO_3 (Platt et al., 1990; Shiraiwa et al., 2009; Knopf et al., 2011). Literature concerning the heterogeneous degradation of pesticides by nitrate radical is very scarce. A few studies (Yang et al., 2011; Liu et al., 2011, 2012, 2015; Wang et al., 2012, 2013; Li et al., 2014) relate the degradation of mainly organophosphorus pesticides according to degradation rates ranging between of 10^{-14} cm^3 $molecule^{-1}$ s^{-1} and 10^{-12} cm^3 $molecule^{-1}$ s^{-1}, which correspond to heterogeneous half-life regarding NO_3 radicals of a few hours. This suggests a significant degradation of pesticides by NO_3 radicals compared to other oxidants. Kinetic studies for the heterogeneous degradation of

pesticides by nitrate radicals are therefore highly needed in order to better understand the role and the importance of this nighttime atmospheric chemistry on pesticide concentrations.

The aim of this study is to investigate the heterogeneous reactivity with NO_3 radicals of eight current-use pesticides (cyprodinil (pyrimidine), deltamethrin (pyrethroid), difenoconazole (triazole), fipronil (pyrazole), oxadiazon (diazole), pendimethalin (dinitroaniline), permethrin (pyrethroid), and tetraconazole (triazole)) adsorbed on hydrophobic silica as a model for mineral atmospheric particles. The compounds under study were selected based on their distribution between gas and particle phases, their toxicity, their presence in the atmosphere (Désert et al., 2018). More, their heterogeneous reactivity was extensively investigated toward OH radicals (Socorro et al., 2016; Mattei et al., 2019a) and ozone (Socorro et al., 2015; Mattei et al., 2018, 2019b). Nitrate radicals exposure experiments were performed using realistic NO_3 radicals concentrations (48 ppt to 635 ppt), temperature (25°C) and relative humidity (40% RH) conditions.

EXPERIMENTAL SECTION

Chemicals

Isoprene (purity > 99.5%) and the eight pesticides (PESTANAL®, analytical standard) : cyprodinil (99.8%), deltamethrin (99.7%), difenoconazole (97.0%), fipronil (97.5%), oxadiazon (99.9%), pendimethalin (98.8%), permethrin (98.3%), and tetraconazole (99.0%) were purchased from Sigma-Aldrich and were used as received. The chemical structures of the pesticides under study are depicted in Supporting Information (SI) Figure S1 and their physicochemical properties are given in SI Table S1.

Silica particles coating

The atmospheric mineral aerosols were mimicked with commercial fumed silica particles (Mattei et al., 2018). In this study, commercial hydrophobic silica particles (AEROSIL R812, Degussa, purity SiO_2 content > 99.8 wt%, mean primary particle size ranges from 5 nm to 50 nm, specific surface area (BET method) of (260 ± 30) $m^2\ g^{-1}$ (Evonik, 2015)) were coated with pesticides according to a liquid/solid adsorption. In an amber Pyrex bulb of 500 cm^3, 600 mg of particles were mixed with 6 mL of a pesticide solution (all 8 pesticides at a concentration of 20 mg L^{-1} in dichloromethane (for HPLC, ≥ 99.8%, Sigma-Aldrich)), i.e., a load of pesticides on silica particles was about 0.02% by weight) and 40 mL of dichloromethane. After a 5-min ultrasound treatment, dichloromethane was evaporated in a rotary evaporator (Rotavapor R-114, Büchi) at 40°C and 850 mbar. This process allows a reproducible coating of the pesticides on the particle's surface (Socorro et al., 2015). Assuming a uniform particle surface coverage for the pesticide molecules and a spherical geometry for particles, the percentage of the particle surface coated with individual pesticide ranged between 0.3% and 0.5% of the monolayer (SI Text S1). Then, the total coated particle surface was 2.8%, which is much less than a monolayer.

Generation of NO_3 radicals and experimental set-up

The gas-phase reaction of ozone in excess with nitrogen dioxide (eq 1) was chosen as the in-situ method to generate NO_3 radicals (Doussin, 2003; Boyd et al., 2015; Nah et al., 2016), measurement of NO_3 radicals concentration was made using isoprene as a tracer (Zhang et al., 2016).

$$O_3 + NO_2 \rightarrow NO_3 + O_2 \qquad k_1 = (3.50 \pm 0.87) \times 10^{-17}\ cm^3\ molecule^{-1}\ s^{-1} \qquad (1)$$

where k_1 is the average rate constant for the reaction of ozone with NO_2 at 298 K (Davis et al., 1974; Graham and Johnston, 1974; Huie and Herron, 1974).

The total gas flow in the reactor was maintained constant at 500 mL min^{-1}. The reaction between NO_2 and O_3 occurred inside the bulb where pesticides were exposed to oxidants

(Figure 1). A constant NO_2 gaseous flow (F1), (F1 to F8, all Brooks SLA Series mass flow controller; accuracy, ±1%) was generated from a gas cylinder (a certified mixture of NO_2 (100 ppm) in Helium, Linde gas 5.0). Successive dilutions of NO_2 flux (from 1 mL min^{-1} to 10 mL min^{-1}) with purified air (zero air generator ZA-1500, F-DGS; F5, 490-499 mL min^{-1}) were made to provide the specified NO_3 radicals concentration. The NO_2 concentrations were monitored continuously online by an Eco Physics model (CLD 88p) associated with an Eco Physics photolytic (metal-halide lamp; 180 W) converter (PLC 860), which allows simultaneous measurements of NO_x, NO_2, and NO concentrations.

Ozone was generated with a constant flow (F3) of 50 mL min^{-1} by passing purified air through an ozone generator (UVP, LLC Upland, UK). Air flow was exposed to ultraviolet (UV) radiation at 185 nm emitted by a mercury vapor pen ray lamp. Each experiment was performed at a constant ozone concentration of $(1.90 \pm 0.15) \times 10^{13}$ molecule cm^{-3} (i.e., (760 ± 60) ppb). The ozone concentrations were monitored continuously online by a photometric ozone analyzer (O_3 41M, Environnement S.A).

A separated humidified air flow was used to avoid a loss of ozone due to its solubility in water. The relative humidity (RH) was adjusted by purified air, which was split into two fluxes. The first one consisted of dry air, while the second one was humidified by bubbling into deionized water. Mixing of these two gas flows (F2, 200 mL min^{-1}) generated a carrier gas at a controlled and constant RH of (40 ± 2)% for all the experiments. 40% RH at 25°C corresponds to a realistic low atmospheric relative humidity level. RH was measured during all the experiments by a hygrometer (Hygrolog NT2" (Rotronic) with a "HygroClip SC04" probe).

600 mg of silica particles coated with pesticides were exposed for 5 hours and 30 mg aliquot of particles were collected at regular intervals during this exposure.

Experimental conditions (concentrations and flow rates) were chosen in order to favor the reactions between NO_2 and O_3 and between NO_3 radicals and isoprene as well as to minimize all other possible reactions such as O_3 with isoprene, NO_2 with isoprene, NO_3 radicals with O_3, or NO_3 radicals with NO_2. Those conditions were chosen with preliminary experiments and with the calculation of the probability for each reaction to occur compared to other possible reactions. All kinetic constants of possible reactions (Table SI2) and the measured concentration of the different species in presence were considered when determining the appropriate concentration conditions for each compound.

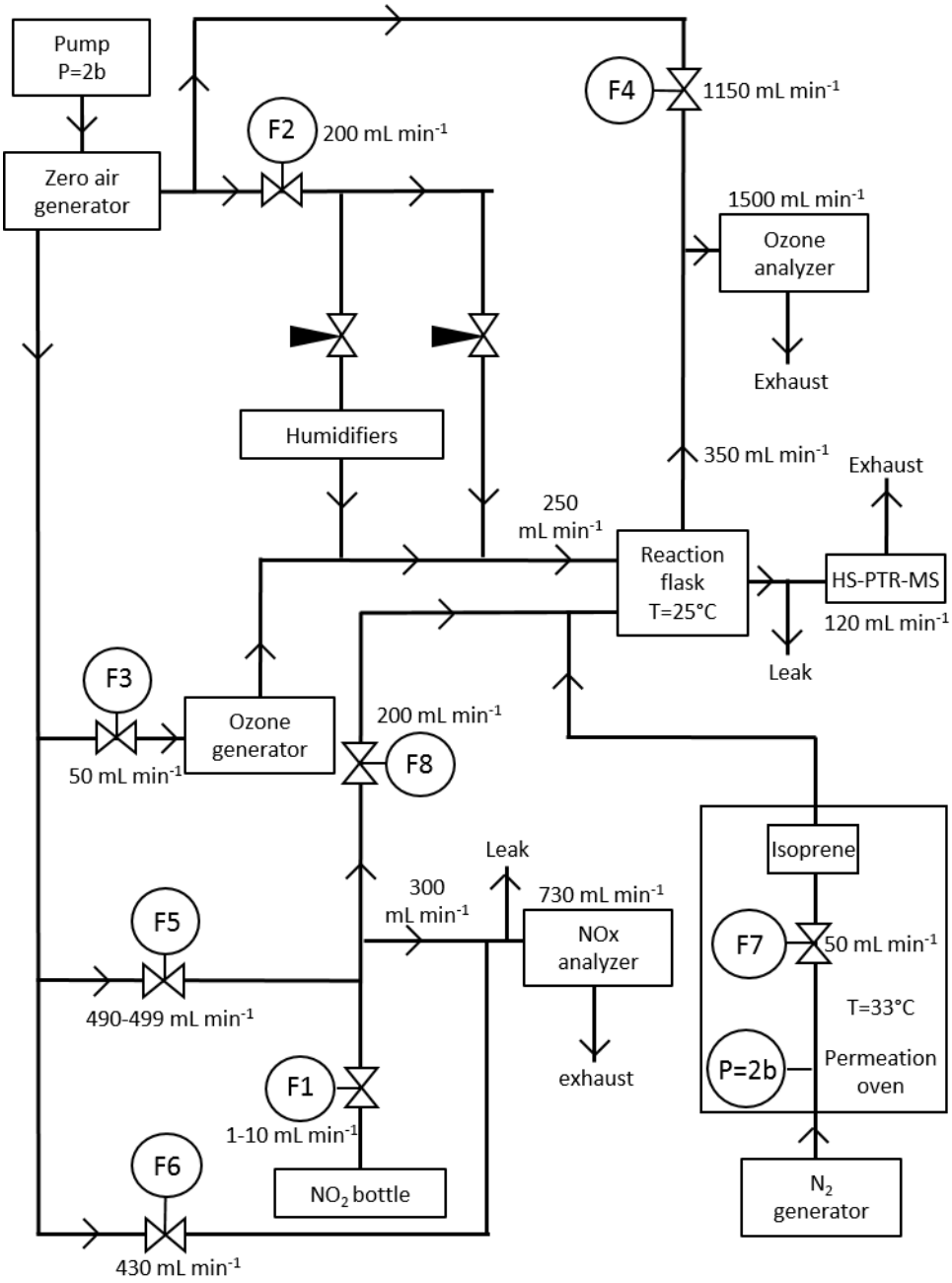

168

169

170 **Figure 1**: Experimental set-up to evaluate the heterogeneous oxidation of adsorbed pesticides

171 under study by NO_3 radicals.

172

173 According to the experimental conditions applied, nitrate radicals concentrations ranged from

174 $(1.19 \pm 0.06) \times 10^9$ molecule cm^{-3} to $(1.59 \pm 0.11) \times 10^{10}$ molecule cm^{-3} (i.e., from 48 to 635

175 ppt). In the atmosphere, NO_3 radicals are predominantly formed by the reaction of nitrogen

dioxide (NO_2) with ozone (O_3). They are photosensitive because of their strong absorption in the visible wavelength region (662 nm) and are therefore absent during daytime but they can greatly accumulate at night. Their nighttime concentration typically ranges between 1 ppt (Geyer et al., 2001; Khan et al., 2008) and 150 ppt (Stutz et al., 2010) (i.e., 2.5×10^7 molecule cm^{-3} and 3.75×10^9 molecule cm^{-3}) and can reach up to 420 ppt (Atkinson et al., 1985), or even 800 ppt (Asaf et al., 2010) (i.e., 2×10^{10} molecule cm^{-3}) in urban polluted areas (Atkinson et al., 1985). Also, it is important to note that experiments were performed using air and not inert atmosphere. This makes the oxidant exposure more realistic as it is known that the presence of O_2 can indirectly influence the degradation mechanism of organic compounds by NO_3 radicals (Docherty and Ziemann, 2006) and might, therefore, influence the kinetics as well.

Indirect measurement of NO_3 radicals

Isoprene was used as a gaseous tracer to determine the NO_3 radicals concentrations (Zhang et al., 2016) (eq 2). It was chosen for its effective and well-described reactivity with NO_3 radicals.

NO_3 + isoprene → Products $\quad k_2 = (6.5 \pm 0.2) \times 10^{-13}\ cm^3\ molecule^{-1}\ s^{-1}$ (2)

where k_2 is the average rate constant for the reaction (Atkinson et al., 1984; Dlugokencky and Howard, 1989; Wille et al., 1991; Berndt and Böge, 1997; Suh et al., 2001; Stabel et al., 2005; Zhao et al., 2011).

Isoprene was generated using a permeation cell, which consisted of a permeable Teflon tube (perfluoroalkoxy, 6.4 mm i.d., 8 cm long) filled with pure isoprene (99%, Sigma-Aldrich) and sealed from both sides. Inside the permeation cell, isoprene was held in liquid/vapor phase equilibrium at 33°C. The Teflon tube was placed in the permeation chamber, a stainless oven equipped with an inlet and outlet allowing a carrier gas flow (dried N_2) to pass through. N_2 was generated by a Domnick Hunter Nitrox UHPLCMS12 nitrogen generator, at 99.5% purity

(0.5% O_2). A pure N_2 constant flow (F7) continuously passed at a rate of 50 mL min^{-1} through the Teflon porous cell to maintain a constant generation.

An HS-PTR-MS (High Sensitivity – Proton Transfer Reaction – Mass Spectrometer, Ionicon Analytik) was used to monitor isoprene (m/z = 69) and its main degradation products (i.e., methacrolein (MACR) and methyl vinyl ketone (MVK), m/z = 71) continuously in gaseous phase inside the bulb reactor with a time resolution of 10 s (Figure S2). Parameters of the HS-PTR-MS during the experiments were as follow: E/N = 144 Td, U_{drift} = 600 V, T_{drift} = 50 °C, P_{drift} = 2.02 mbar. U_{drift} is the electric potential applied to the drift tube; T_{drift} and P_{drift} are the temperature and the pressure in the drift tube, respectively. E is the strength of the electrical field in V cm^{-1} and N is the gas number density in cm^3. The ratio E/N in Townsend (1 Townsend = 10^{-17} cm^2 V^{-1}) is a defining characteristic of the drift tube.

Isoprene reacts in the bulb with NO_3 radicals (eq 2), but can also react with O_3 (eq 3), and NO_2 (eq 4) as follows:

O_3 + isoprene → Products $k_3 = (9.6 \pm 0.7) \times 10^{-18}$ cm^3 $molecule^{-1}$ s^{-1} (3)

NO_2 + isoprene → Products $k_4 = (10.3 \pm 0.3) \times 10^{-20}$ cm^3 $molecule^{-1}$ s^{-1} (4)

where k_3 and k_4 are the rate constants for the reaction of isoprene with O_3 (Karl et al., 2004) and NO_2 (Atkinson et al., 1984), respectively.

The NO_3 radical concentrations were determined using the consumption of the tracer (isoprene) as follows:

$$-\frac{d[isoprene]}{dt} = k_2 \times [isoprene] \times [NO_3] + k_3 \times [isoprene] \times [O_3] + k_4 \times [isoprene] \times [NO_2] \quad (5)$$

The integration of eq 5 gives the eq 6 which makes it possible to calculate NO_3 radical concentrations in the reactor all along with experiments.

$$[NO_3] = \ln\left(\frac{[isoprene]_0}{[isoprene]_t}\right) \times \frac{1}{k_2 \times t} - (k_3 \times [O_3] - k_4 \times [NO_2]) \times \frac{1}{k_2} \quad (6)$$

Where t (s) is the residence time of compounds in the gaseous phase in the bulb, $[isoprene]_0$ and $[isoprene]_t$ (molecule cm^{-3}) are the initial (in absence of oxidants) and the measured concentrations of isoprene in the bulb reactor at time t, respectively, finally k_2 is the rate constant of the reaction between isoprene and NO_3 radicals (eq 2), k_3 is the rate constant of the reaction between isoprene and O_3 (eq 3), and k_4 is the rate constant of the reaction between isoprene and NO_2 (eq 4).

Extraction and pesticides quantification

During exposure, 30 mg aliquots of particles were regularly sampled in order to quantify the remaining adsorbed pesticides on their surface. Each 30 mg aliquot of particles was individually extracted by accelerated solvent extraction (ASE 350, Dionex) with dichloromethane. For this purpose, particles were introduced in a 33 mL stainless steel cell with an internal standard solution (Triphenyl phosphate, 99.9%, Sigma-Aldrich). Afterward, the extracts were concentrated under a nitrogen flow using a concentration workstation (TurboVap II, Biotage).

Analyses of the obtained solutions were realized using gas chromatography coupled to tandem mass spectrometry (GC/MS-MS), with a Trace GC Ultra (Thermo Scientific) coupled to a TSQ Quantum™ Triple Quadrupole (Thermo Scientific) using electron impact ionization (70 eV).

More details about ASE extraction, concentration, and GC/MS-MS analysis are available elsewhere (Socorro et al., 2015).

Determination of first-order rate constants

To obtain the first-order rate constants $k^I_{NO_{3(part)}}$ for the heterogeneous reactions of NO_3 radicals with a pesticide, the following procedure was applied:

248 $\text{Pesticide}_{\text{ads}} + NO_3 \rightarrow \text{Products}$ (7)

249 All degradation reactions of a pesticide not initiated by NO_3 radicals are defined as follows:

250 $\text{Pesticide}_{\text{ads}} + Y \rightarrow \text{Products}$ (8)

251 where Y represent all residual oxidant species. Y species include ozone, nitrogen dioxide but
252 also eventual compounds or radicals formed by side reactions. For instance, the reactivity of
253 NO_3 radicals with unsaturated volatile organic compounds could lead to the formation of HO_2
254 or OH radicals (Canosa-Mas et al., 1999; Salisbury, 2001). Also the combination of NO_3
255 radical and NO_2 could lead to the formation of N_2O_5 which is known to be heterogeneously
256 reactive with organic compounds (Knopf et al., 2011). However, according to the
257 concentrations of NO_2 and NO_3 in the reactor and the kinetic constants (Table SI2) leading to
258 the formation of N_2O_5, the formation of N_2O_5 is very unlikely.

259 The reaction rate of the pesticide under study versus time is then defined by Eq 10.

260 $$-\frac{d[Pesticide_{ads}]}{dt} = k^{II}_{NO_{3(part)}} \times [Pesticide_{ads}] \times [NO_3] + k^{I}_{des_{(part)}} \times [Pesticide_{ads}] +$$

261 $$k^{I}_{hydr_{(part)}} \times [Pesticide_{ads}] + k^{II}_{Y_{(part)}} \times [Pesticide_{ads}] \times [Y] \quad (9)$$

262 where $k^{II}_{NO_{3(part)}}$ and $k^{II}_{Y_{(part)}}$ (cm^3 $molecule^{-1}$ s^{-1}) are the second-order rate constants of the
263 heterogeneous reactions with NO_3 radicals and all other species different than NO_3 radicals,
264 respectively. $k^{I}_{des_{(part)}}$ (s^{-1}) is the first order kinetic desorption rate constant and $k^{I}_{hydr_{(part)}}$ (s^{-1}) is the pseudo-first-order kinetic hydrolysis rate constant.

266 The integration of eq 10 leads to:

267 $$ln\left(\frac{[Pesticide_{ads}]_t}{[Pesticide_{ads}]_0}\right) = -(k^{I}_{NO_{3(part)}} + k^{I}_{des_{(part)}} + k^{I}_{hydr_{(part)}} + k^{I}_{Y_{(part)}}) \times t = -k^{I}_{all_{(part)}} \times t$$

268 (10)

where $k^{I}_{all_{(part)}}$ (s^{-1}) is the pseudo-first-order constant of the heterogeneous reactions with NO_3 radicals and other species different than NO_3 radicals (Y species), as well as the pesticide loss due to hydrolysis or desorption. $k^{I}_{all_{(part)}}$ is experimentally determined as the slope of the Napierian logarithm of normalized pesticide concentration's decay versus the exposure time.

Considering that NO_3 radicals are continuously produced in the reactor, a pseudo-first-order reaction rate constant $k^{I}_{NO3_{(part)}}$ was assumed and is expressed as follows:

$$k^{I}_{NO3_{(part)}} = k^{I}_{all_{(part)}} - k^{I}_{des_{(part)}} - k^{I}_{hydr_{(part)}} - k^{II}_{Y_{(part)}} \times [Y] \qquad (11)$$

($k^{I}_{des_{(part)}}$ + $k^{I}_{hydr_{(part)}}$) were determined experimentally in the absence of oxidants (Mattei et al., 2018) while $k^{I}_{Y_{(part)}}$ was determined mathematically as the intercept of the slope fitting $k^{I}_{all_{(part)}}$ versus $[NO_3]$ after correction form the corresponding ozonolysis rate constant.

Kinetic mechanism model

In order to determine kinetic constants that are independent of the NO_3 radical concentration, pseudo-first-order kinetic constants were plotted against the NO_3 radical concentration. Two fitting methods were used: Langmuir–Rideal (L-R, also known as Eley-Rideal) fitting models linearly the reaction between a reactant in the gas phase with one adsorbed on the surface of the particles whereas Langmuir–Hinshelwood (L-H) models non-linearly the reaction between two reactants adsorbed on the surface.

The second-order kinetic constant $k^{II}_{NO_{3(part)}}$ (cm^3 $molecule^{-1}$ s^{-1}) determined with L-R fitting correspond to the slope of the linear regression line fitting the first order kinetic constant according to the oxidant concentration. This correspond to eq 13:

$$k^{II}_{NO_{3(part)}} = \frac{k^{I}_{NO_3}}{[NO_3]} \qquad (12)$$

Half-lives corresponding to an L-R model can be calculated as follow:

$$t_{½\,NO_3(\text{part})} = \frac{ln2}{k^{II}_{NO_3(part)} \times [NO_3]} \quad (13)$$

Where $t_{½\,NO_3(\text{part})}$ (s^{-1}) is the half-life of a pesticide and $[NO_3]$ (molecules cm^{-3}) is the atmospheric concentration of NO_3 radicals chosen as representative of atmospheric values. In this work, $[NO_3]$ used is 5×10^8 molecule cm^{-3} (i.e., 20 ppt) over an exposure time of 12 hours (Atkinson, 1991).

With the L-H model, the pseudo-first-order rate coefficient ($k^I_{NO_3}$, s^{-1}) is expressed using eq 15:

$$k^I_{NO_3} = \frac{(k_{max} \times k_{NO_3} \times [NO_3])}{(1 + k_{NO_3} \times [NO_3])} \quad (14)$$

where k_{max} (s^{-1}) is the maximum rate constant obtained at high oxidant concentration and k_{NO_3} (molecule cm^{-3}) is the NO_3 radical gas-surface equilibrium constant. These two parameters can be obtained by fitting the experimental results $k^I_{NO_3}$ versus [NO_3] using a non-linear least-square fit of eq 15. Hence, the second-order rate constant of the reaction follows a non-linear dependence with respect to the gas-phase oxidant.

Uncertainties were determined as the error on the fitting parameters calculated by the software Igor Pro, taking into account both the uncertainties on the first-order kinetic constants and the nitrate radical concentration.

Half-lives corresponding to an L-H model is calculated as follow:

$$t_{½\,NO_3(\text{part})} = \frac{ln2}{k^I_{NO_3}} \quad (15)$$

Using ($k^I_{NO_3}$, s^{-1}) calculated for [NO_3] of 5×10^8 molecule cm^{-3} and an exposure time of 12 h, as presented previously.

RESULTS AND DISCUSSION

Heterogeneous reactivity kinetics

Oxidation experiments were conducted for five nitrate radicals concentrations (i.e., $(1.2 \pm 0.1) \times 10^9$; $(1.3 \pm 0.1) \times 10^9$; $(4.9 \pm 0.2) \times 10^9$; $(8.6 \pm 0.6) \times 10^9$ and $(1.6 \pm 0.1) \times 10^{10}$ molecule cm^{-3}) in order to evaluate the heterogeneous degradation rates of 8 pesticides, i.e., deltamethrin, permethrin, fipronil, tetraconazole, oxadiazon, cyprodinil, pendimethalin, and difenoconazole, adsorbed on silica particles.

Under these experimental conditions, all pesticides under study showed significant degradation, in decreasing order of reactivity: tetraconazole ~ permethrin > oxadiazon ~ cyprodinil > fipronil ~ deltamethrin ~ pendimethalin according to an L-R model and tetraconazole > permethrin ~ deltamethrin > pendimethalin > fipronil > cyprodinil ~ oxadiazon according to an L-H model. Within 5h of exposure to nitrate radicals ranging from $(1.2 \pm 0.1) \times 10^9$ molecule cm^{-3} to $(1.6 \pm 0.1) \times 10^{10}$ molecule cm^{-3}, tetraconazole degradation ranged from 29% to 61% of the initial concentration. Difenoconazole was also degraded by nitrate radicals, nevertheless from the noisy data obtained, it is not possible to determine kinetic constants. Therefore, results regarding difenoconazole degradation are not presented thereafter.

Pseudo-first-order constants corresponding to the degradation of pesticides by nitrate radicals were plotted against the nitrate radical concentrations (Figure 2). Pseudo-first-order kinetic constants for all pesticides under study increased as expected with an increase of nitrate radicals concentrations (Figure 2).

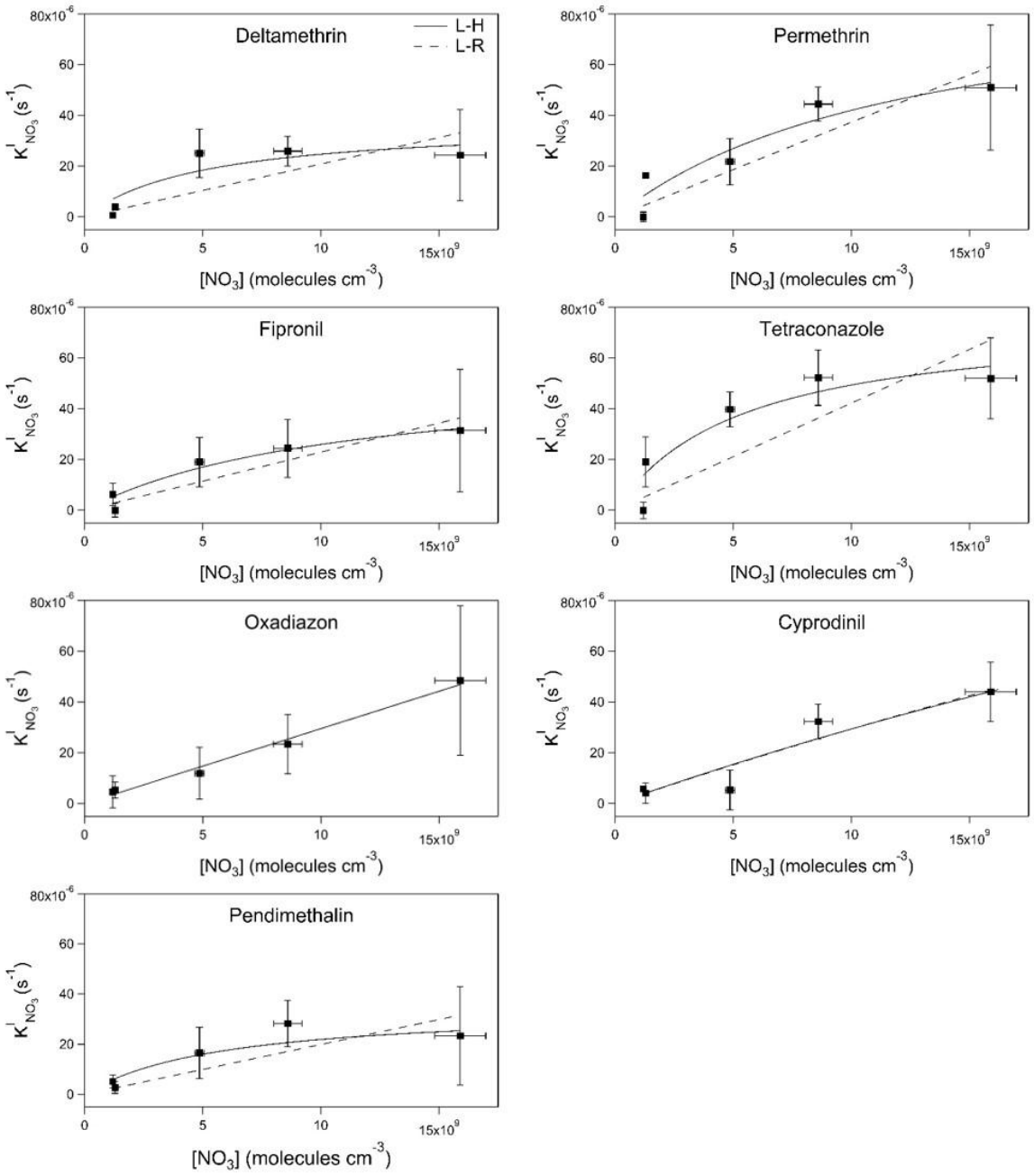

Figure 2: Pseudo-first-order kinetic constants for the degradation of pesticides adsorbed on hydrophobic silica by nitrate radicals at 40% RH at five nitrate radicals concentrations from (1.2 ± 0.1) × 10^{9} molecule cm^{-3} to (1.6 ± 0.1) × 10^{10} molecule cm^{-3}. The solid line corresponds to an L-H fitting and the dotted line corresponds to an L-R fitting.

Kinetic mechanism model

The different reaction rate constants of heterogeneous oxidation of the seven adsorbed pesticides by nitrate radicals, described by L-R and L-H mechanisms, as well as the

corresponding half-lives are summarized in Table 1. For all pesticides, both L-R and L-H patterns can be applied although, for most compounds, the L-H model seems to better fit the experimental data. However, the L-H model leads to greater uncertainties on the second order kinetic constants than the L-R model. According to an L-R model, the slowest degradation rate is obtained for pendimethalin with $k^{II}_{NO_3(part)}$ = (1.99 ± 0.42) × 10^{-15} cm^3 $molecule^{-1}$ s^{-1} and the fastest degradation rate is obtained for tetraconazole with $k^{II}_{NO_3(part)}$ = (4.22 ± 0.87) × 10^{-15} cm^3 $molecule^{-1}$ s^{-1}. According to an L-H model, kinetic constants vary from k_{max} = (1.71 ± 1.69) × 10^{-2} s^{-1} and k_{NO_3} = (1.72 ± 1.70) × 10^{-13} cm^3 $molecule^{-1}$ for oxadiazon to k_{max} = (7.59 ± 2.36) × 10^{-5} s^{-1} to k_{NO_3} = (1.85 ± 1.43) × 10^{-10} cm^3 $molecule^{-1}$ for tetraconazole.

Kinetic data obtained in this study are compared to the literature. Unfortunately, because of the lack of data, these comparisons are done only with other pesticides. Literature data about the heterogeneous degradation of pesticides by NO_3 radicals (Yang et al., 2011; Liu et al., 2012, 2014, 2015; Wang et al., 2012, 2013; Li et al., 2014) only considered the L-R mechanism. The heterogeneous reactivity of organic compounds with hydroxyl radicals was described by both L-H mechanism (Bagot et al., 2008; Vlasenko et al., 2008; Enami et al., 2014) and L-R mechanism (Socorro et al., 2016). However, L-R mechanism was explained partly because of OH radicals' really short lifetime which does not allow the necessary time to adsorb on the surface (Socorro et al., 2016). NO_3 radicals have a much longer lifetime than OH radicals, in the order of magnitude of the minute (Platt et al., 1984) versus the second (Gligorovski et al., 2015), respectively. NO_3 radicals may be able to adsorb on the particle surface before reacting with pesticides allowing an L-H mechanism.

Comparison with other pesticides in the particle-phase

362 Table 1: Kinetic data for the heterogeneous reactivity of NO_3 radicals with the adsorbed pesticides under study (in bold) and corresponding

363 atmospheric half-lives, as well as literature data for the degradation of other pesticides by NO_3 radicals

Chemical Family	Pesticide	Relative humidity (%)	Temperature (°C)	NO_3 radical concentration (molecule cm^{-3})	Surface	Langmuir - Rideal model		Langmuir - Hinshelwood model			Reference
						$k^{II}_{NO_{3(part)}}$ (cm^3 $molecule^{-1}$ s^{-1})	$t_{½\ NO_{3(part)}}$ (d)	$k_{(max)}$ (s^{-1})	K_{NO3} (cm^3 $molecule^{-1}$)	$t_{½\ NO_{3(part)}}$ (d)	
Carbamate	Carbaryl	~ 10	25	Unknown	Azelaic acid	4.4×10^{-13}	0.7	/			Yang et al. (2011)
Dinitroaniline	**Pendimethalin**	**40 ± 2**	**25 ± 1**	**$(1.2 – 16.0) \times 10^9$**	**Hydrophobic silica**	**$(1.99 \pm 0.42) \times 10^{-15}$**	**16.1**	**$(3.47 \pm 1.33) \times 10^{-5}$**	**$(1.71 \pm 1.57) \times 10^{-10}$**	**5.6**	**This work**
Organophosphorus	Chlorpyrifos	~ 40	~ 15	$(5.0 \pm 0.3) \times 10^{10}$	Azelaic acid	$(3.4 \pm 0.2) \times 10^{-12}$	0.09	/			Li et al. (2014)
	Fenthion	~ 5	~ 20	$10^{11} – 10^{12}$	Azelaic acid	$3.3 \times 10^{-14} – 3.3 \times 10^{-13}$	0.9 – 9.3	/			Liu et al. (2012)
	Malathion	~ 5	~ 20	$10^{11} – 10^{12}$	Azelaic acid	$5.6 \times 10^{-14} – 5.6 \times 10^{-13}$	0.6 – 5.5	/			Liu et al. (2012)
	Parathion	~ 5	~ 20	$10^{11} – 10^{12}$	Azelaic acid	$5.5 \times 10^{-15} – 5.5 \times 10^{-14}$	5.6 – 56	/			Liu et al. (2012)
	Parathion	~ 5	~ 20	$(2.7 – 8.5) \times 10^9$	Azelaic acid	$(2.97 \pm 0.13) \times 10^{-12}$	0.1	/			Liu et al. (2015)
	Phosmet	~ 5	~ 20	$10^{11} – 10^{12}$	Azelaic acid	$(1.92 \pm 0.09) \times 10^{-12}$	0.2	/			Liu et al. (2011)
	Phosmet	~ 5	~ 20	$(2.7 – 8.5) \times 10^9$	Azelaic acid	$(2.80 \pm 0.16) \times 10^{-12}$	0.1	/			Liu et al. (2015)
Oxadiazole	**Oxadiazon**	**40 ± 2**	**25 ± 1**	**$(1.2 – 16.0) \times 10^9$**	**Hydrophobic silica**	**$(2.95 \pm 0.12) \times 10^{-15}$**	**10.9**	**$(1.71 \pm 1.69) \times 10^{-2}$**	**$(1.72 \pm 1.70) \times 10^{-13}$**	**10.9**	**This work**
Pyrazole	**Fipronil**	**40 ± 2**	**25 ± 1**	**$(1.2 – 16.0) \times 10^9$**	**Hydrophobic silica**	**$(2.29 \pm 0.31) \times 10^{-15}$**	**14**	**$(5.45 \pm 1.89) \times 10^{-5}$**	**$(9.05 \pm 5.97) \times 10^{-11}$**	**6.7**	**This work**

Pyrethroid	**Deltamethrin**	**40 ± 2**	**25 ± 1**	**(1.2 – 16.0) × 10^9**	**Hydrophobic silica**	**(2.08 ± 0.51) × 10^{-15}**	**15.4**	**(3.75 ± 1.52) × 10^{-5}**	**(1.93 ± 1.98) × 10^{-10}**	**4.6**	**This work**
	Fenvalerate	~ 5	~ 25	(1.5 – 10.2) × 10^9	Azelaic acid	(1.86 ± 0.04) × 10^{-12}	0.2	/			Wang et al. (2013)
	Permethrin	**40 ± 2**	**25 ± 1**	**(1.2 – 16.0) × 10^9**	**Hydrophobic silica**	**(3.73 ± 0.52) × 10^{-15}**	**8.6**	**(9.48 ± 4.75) × 10^{-5}**	**(7.93 ± 7.21) × 10^{-11}**	**4.4**	**This work**
	Phenothrin	~ 5	~ 25	(1.5 – 10.2) × 10^9	Azelaic acid	(1.61 ± 0.03) × 10^{-12}	0.2	/			Wang et al. (2013)
	Resmethrin	~ 5	~ 25	(1.5 – 10.2) × 10^9	Azelaic acid	(5.54 ± 0.14) × 10^{-12}	0.1	/			Wang et al. (2013)
Pyrimidine	**Cyprodinil**	**(0-80) ± 2**	**25 ± 1**	**(1.2 – 16.0) × 10^9**	**Hydrophobic silica**	**(2.87 ± 0.32) × 10^{-15}**	**11.2**	**(0.39 ± 1.62) × 10^{-3}**	**(0.81 ± 3.70) × 10^{-11}**	**10.1**	**This work**
	Pyrimicarb	~ 10	~ 25	(0.6 – 7.0) × 10^9	Azelaic acid	(7.5 ± 0.3) × 10^{-13}	0.4	/			Wang et al. (2012)
	Pirimophos-methyl	~ 10	~ 25	(0.6 – 7.0) × 10^9	Azelaic acid	(9.9 ± 0.3) × 10^{-12}	0.03	/			Wang et al. (2012)
Triazine	Ametryn	~ 5	~ 25	(0.7 – 7.9) × 10^{10}	Azelaic acid	8.4 × 10^{-13}	0.4	/			Liu et al. (2014)
Triazole	**Difenoconazole**	**40 ± 2**	**25 ± 1**	**(1.2 – 16.0) × 10^9**	**Hydrophobic silica**	**/**	**/**	**/**			**This work**
	Tetraconazole	**40 ± 2**	**25 ± 1**	**(1.2 – 16.0) × 10^9**	**Hydrophobic silica**	**(4.22 ± 0.69) × 10^{-15}**	**7.6**	**(7.59 ± 2.36) × 10^{-5}**	**(1.85 ± 1.43) × 10^{-10}**	**2.4**	**This work**

364 Atmospheric half-lives calculated for an average concentration $[NO_3]_{(gas)}$ = 5 × 10^8 molecule cm^{-3} and for an exposure of 12 h per day (Atkinson, 1991).

365

Some studies about heterogeneous NO_3 radicals oxidation of pesticides exist, in which kinetic data were obtained with pesticides suspended with azelaic acid as nucleation cores to form aerosols exposed to NO_3 radicals give second-order rate constants ranged between 10^{-14} cm^3 $molecule^{-1}$ s^{-1} and 10^{-12} cm^3 $molecule^{-1}$ s^{-1} (Yang et al., 2011; Liu et al., 2012, 2014, 2015; Wang et al., 2012, 2013; Li et al., 2014). These values are higher than the second-order rate constants obtained in this study (about 10^{-15} cm^3 $molecule^{-1}$ s^{-1}). Beyond the nature of the pesticides under study, the relative humidity could explain this difference. Literature data were obtained at low relative humidity (5-10% RH, except one at 60% RH) (Yang et al., 2011; Liu et al., 2012, 2014; Wang et al., 2012, 2013; Li et al., 2014) giving second-order rate constants ranging between 10^{-14} cm^3 $molecule^{-1}$ s^{-1} and 10^{-12} cm^3 $molecule^{-1}$ s^{-1}. Previous work highlighted that the heterogeneous reactivity of organic compounds including pesticides with ozone was fastest when the relative humidity decreased (Pöschl et al., 2001; Kaiser et al., 2011; Mattei et al., 2018). This phenomenon was attributed to the absence or low competition between water and pesticide molecules to react with the oxidant at low relative humidity. As this present work was conducted at 40% RH, it is possible that part of the differences in the degradation rates obtained is due to this difference in experimental conditions.

However, an other experimental condition should lead to opposite results. According to the experimental process described in the literature (Yang et al., 2011; Liu et al., 2012, 2014, 2015; Wang et al., 2012, 2013; Li et al., 2014), pesticides were suspended on an azelaic nucleation core which leads to particles highly concentrated in pesticides whereas, in the present study, the total coated surface of silica particles was less than a monolayer (3% of a monolayer). The high pesticide concentrations in the aerosols used by the authors previously cited should lead to slower reactivity than in the case of pesticides adsorbed on the aerosol surface. Indeed, it was previously demonstrated that NO_3 radicals only react with the top few

molecular surface layers of a substrate (Moise et al., 2002). In addition, heterogeneous reactivity was shown to be slowed down by particle's surface coating increase due to the decrease of accessibility of pesticides for the oxidant. This phenomenon was demonstrated for heterogeneous degradation of pesticides by ozone (El Masri et al., 2016).

Reaction pathways

All pesticides under study were degraded by NO_3 radicals. From a mechanistic point of view, the nitration of a double bond (electrophilic addition of NO_3 radical, followed by an addition of NO_2 molecule and an elimination of HNO_3 molecule, leading to the formation of a NO2 moiety), which is favored on the aromatic ring (Wang et al., 2013), is a common reaction pathway. As all the pesticides under study are aromatic organic compounds (Figure S1), they could all react in this way. Other studies on the heterogeneous reactivity between NO_3 radicals and pesticides of the pyrethroid family, as deltamethrin and permethrin, also suggested the ester cleavage, as shown for resmethrin (Wang et al., 2013) and the NO_3 radicals addition to an aliphatic double bond, as shown for phenothrin (Wang et al., 2013). Liu et al., (2014) also proposed the oxidation by NO_3 radicals of the sulfur atom on a methyl sulfoxide group for fenthion and ametryn. The trifluoro sulfoxide group available on fipronil could be similarly oxidized.

Comparison with pesticide's degradation in the gas-phase

In the literature, some kinetic data are available for the degradation of pesticides in the gas phase, even if no data concerns the chemical families of compounds under study.

Table 2: Kinetic data available in the literature for the gaseous reactivity of NO_3 radicals of pesticides and corresponding atmospheric half-lives. None of the references provided RH data.

Chemical Family	Pesticide	Temperature (°C)	$k^{II}_{NO_{3(part)}}$ (cm^3 $molecule^{-1}$ s^{-1})	$t_{½\ NO_{3(part)}}$ (d)	Reference

Carbamate	Carbaryl[a]	25	3.37×10^{-13}	0.1	Cheng et al. (2017)
Organochlorine	DDT[a]	25	4.01×10^{-15}	8.0	Liu et al. (2014)
Organophosphorus	DEEP[b]	25 ± 2	$(3.4 \pm 1.4) \times 10^{-16}$	94.4	Aschmann et al. (2005a)
	DEMP[b]	25 ± 2	$(3.7 \pm 1.1) \times 10^{-16}$	86.7	Aschmann et al. (2005a)
	DEMPT[b]	23 ± 2	$(2.01 \pm 0.20) \times 10^{-15}$	16.0	Aschmann et al. (2006)
	DMEP[b]	25 ± 2	$(3.4 \pm 1.4) \times 10^{-16}$	94.4	Aschmann et al. (2005b)
	DMHP[b]	25 ± 2	$< 1.4 \times 10^{-16}$	> 229.2	Aschmann et al. (2005b)
	DMMP[b]	25 ± 2	$(2.0 \pm 1.0) \times 10^{-16}$	160.5	Aschmann et al. (2005b)
	IMMP[b]	23 ± 2	$(4.8 \pm 2.1) \times 10^{-16}$	66.9	Aschmann et al. (2010)
	TEP[b]	25 ± 2	$(2.4 \pm 1.4) \times 10^{-16}$	133.7	Aschmann et al. (2005a)
	TEPT[b]	23 ± 2	$(1.03 \pm 0.10) \times 10^{-15}$	31.2	Aschmann et al. (2006)
	TMP[b]	25 ± 2	$< 3 \times 10^{-14}$	> 1.1	Goodman et al. (1988)

DDT : 1,1'-(2,2,2-trichloroethylidene)bis[4-chlorobenzene] ; DEEP : DiEthyl EthylPhosphonate ; DEMP : DiEthyl MethylPhosphonate ; DEMPT : *O*,*O*-DiEthyl MethylPhosphonoThioate ; DMEP : DiMethyl EthylPhosphonate ; DMHP : DiMethyl Phosphonate ; DMMP : DiMethyl MethylPhosphonate ; IMMP : Isopropyl Methyl Methylphosphonate ; TEP : TriEthyl Phosphate ; TEPT : *O*,*O*,*O*-TriEthyl PhosphonoThioate ; TMP : Trimethyl Phosphorothioates

[a] NO_3 radicals concentration calculated theoretically, [b] NO_3 radicals concentration unknown

Atmospheric half-lives calculated for an average concentration $[NO_3]_{(gas)} = 5 \times 10^8$ molecule cm^{-3} and for an exposure of 12 h per day (Atkinson, 1991)

Degradation rate constants measured or modeled for pesticides in the gas-phase exposed to NO_3 radicals range from 10^{-13} cm^3 molecule^{-1} s^{-1} to 10^{-16} cm^3 molecule^{-1} s^{-1} (Table 2) (Goodman et al., 1988; Aschmann et al., 2005a, 2005b; Aschmann and Atkinson, 2006; Liu et al., 2014; Cheng et al., 2017). Heterogeneous reactivity showed degradation rate constants of about 10^{-15} cm^3 molecule^{-1} s^{-1} (this study). These differences in degradation rates between gas-phase and particle-phase were expected. Indeed, pesticide's degradation has been demonstrated to be different in the particle-phase and in the gas-phase in case of their degradation by OH radicals (Socorro et al., 2016), as well as by ozone (Socorro et al., 2015).

Comparison with the degradation mechanism by OH radicals

NO_3 radicals typically react with organic compounds by electrophilic addition onto aliphatic or aromatic double bond (Knopf et al., 2011; Liu et al., 2012; Lauraguais et al., 2016; Zhang et al., 2016) or via an H-abstraction although this second mechanism is generally less favored (Wayne et al., 1991; Finlayson-Pitts and Pitts, 2009). Those mechanisms are the same as those governing the reactivity with OH radicals (George and Abbatt, 2010; Borrás et al., 2015). Both of those mechanisms are likely to happen on the pesticides under study, considering their molecular structure (Figure S1). Yet, while this work shows the effective heterogeneous degradation of all pesticides under study by nitrate radicals, only four of them (cyprodinil, deltamethrin, permethrin, and pendimethalin) were heterogeneously degraded by OH radicals in similar experimental conditions (i.e., RH and hydrophobic silica particles) (Socorro et al., 2016). This difference in reactivity despite the similarity of the mechanisms could be the result of the longer life time of nitrate radicals compared to the hydroxyl radicals, leading to differences in diffusion velocity of radicals, which allows some pesticides to be accessible to nitrate radicals. Additionally, even though the mechanism is similar in theory, their probability to occur on a given molecular function might differ according to the oxidant. For instance, triazole reactivity toward OH radicals in the gas phase is considered as a very slow reaction at ambient temperature (Derbel et al., 2018), which might explain the non-degradation of tetraconazole and difenoconazole with OH radicals, however, tetraconazole is the fastest degraded pesticide by NO_3 radicals, showing that the probability of reactions are different between OH and NO_3 radicals.

Atmospheric implications

Second-order rate constants calculated for the heterogeneous reactivity of pesticides under study with NO_3 radicals were of the order of magnitude of 10^{-15} cm^3 $molecule^{-1}$ s^{-1}, which is faster than those obtained for the heterogeneous reactivity of the same pesticides with ozone (i.e., $k^{II}_{NO_3(part)}$ ~ 10^{-18} cm^3 $molecule^{-1}$ s^{-1}) (Mattei et al., 2018) but slower than those obtained

for the heterogeneous reactivity with OH radicals (i.e., $k^{II}_{OH_{(part)}}$~ 10^{-12} cm^3 $molecule^{-1}$ s^{-1}) (Socorro et al., 2016). Thus, NO_3 radicals can have a significant influence on the atmospheric fate of pesticides in particle-phase.

Considering an average NO_3 radicals concentration of 20 ppt over 12 hours (Atkinson, 1991), the half-lives in particle-phase regarding NO_3 radical oxidation calculated for the pesticides under study vary from 7.6 days (tetraconazole) to 16.1 days (pendimethalin) for an L-R mechanism, and from 2.4 day (tetraconazole) to 10.9 days (oxadiazon) for an L-H mechanism (Table 1). Half-lives previously measured for the same pesticides varied from 0.4 days to 91 days for ozone (40 ppb, 24/24 h exposure) (Mattei et al., 2018) and from 0.1 days to 9 days for OH radicals (0.06 ppt, 12/24 h exposure) (Socorro et al., 2016). The comparison of those order of magnitude is in accordance with the literature available on the reactivity of other volatile organic compounds, such as polycyclic aromatic compounds, assessing that the heterogeneous reactivity with NO_3 radicals is at least as important as the heterogeneous reactivity with OH radicals or ozone (Shiraiwa et al., 2009; Kaiser et al., 2011).

These half-lives in particle-phase of difenoconazole, tetraconazole, fipronil, oxadiazon, deltamethrin, cyprodinil, permethrin, and pendimethalin, imply that these pesticides can be transported over long distances, reaching remote regions all over the world. Obtained values show that atmospheric heterogeneous degradation of pesticides, and in a greater extent of semi-volatile organic compounds, is of significant importance for nighttime atmospheric chemistry processes.

In this study, the heterogeneous reactivity of pesticides was investigated on model silica particles. However, NO_3 radicals uptake on surfaces depend on the substrate nature (Moise et al., 2002; Karagulian and J. Rossi, 2005; Gross et al., 2009) and reactive uptake of NO_3 radicals on organic surfaces can vary by three orders of magnitude according to the surface

type (George and Abbatt, 2010). Moreover, experiments were conducted only at 40% RH, but the relative humidity level could also change the degradation rates indirectly by influencing the uptake of NO_3 radicals by competition mechanisms, as heterogeneous reactivity degradation by ozone was already described as dependent on the relative humidity (Pöschl et al., 2001; Kaiser et al., 2011; Mattei et al., 2018).

Finally, it is expected that degradation of the pesticides under study leads to the formation of nitrogenated compounds such as hydroxyl nitrate or carbonylnitrate compounds through nitrooxyradicals intermediates or to the formation of a carbonyl or hydroxyl-substituted compounds (Kwok et al., 1995; Perring et al., 2009). These degradation products were not detected in samples possibly because of their thermolability, their volatilization or their too low concentrations. As observed for the heterogeneous degradation of the same pesticides by ozone (Socorro et al., 2016), the degradation products can be of different health and environmental effects than the parent pesticides. They should be included in the evaluation studies of air quality.

ACKNOWLEDGMENTS

This work has been carried out thanks to the support of the COPP'R project "Modelling of atmospheric contamination by plant protection products at the regional scale" funded by the PRIMEQUAL – AGRIQA « Agriculture et qualité de l'air » program. C. Mattei received a doctoral grant from the French Environment and Energy Management Agency (ADEME) and the Region Provence-Alpes-Côte d'Azur.

REFERENCES

Asaf, D., Tas, E., Pedersen, D., Peleg, M., Luria, M., 2010. Long-Term Measurements of NO3 Radical at a Semiarid Urban Site: 2. Seasonal Trends and Loss Mechanisms. Environ. Sci. Technol. 44, 5901–5907. https://doi.org/10.1021/es100967z

Aschmann, S.M., Atkinson, R., 2006. Kinetic and Product Study of the Gas-Phase Reactions of OH Radicals, NO3 Radicals, and O3 with (C2H5O)2P(S)CH3 and (C2H5O)3PS. J. Phys. Chem. A 110, 13029–13035. https://doi.org/10.1021/jp065382v

Aschmann, S.M., Tuazon, E.C., Atkinson, R., 2005a. Atmospheric Chemistry of Dimethyl Phosphonate, Dimethyl Methylphosphonate, and Dimethyl Ethylphosphonate. J. Phys. Chem. A 109, 11828–11836. https://doi.org/10.1021/jp055286e

Aschmann, S.M., Tuazon, E.C., Atkinson, R., 2005b. Atmospheric Chemistry of Diethyl Methylphosphonate, Diethyl Ethylphosphonate, and Triethyl Phosphate. J. Phys. Chem. A 109, 2282–2291. https://doi.org/10.1021/jp0446938

Atkinson, R., 1991. Kinetics and Mechanisms of the Gas-Phase Reactions of the NO3 Radical with Organic Compounds. J. Phys. Chem. Ref. Data 20, 459–507. https://doi.org/10.1063/1.555887

Atkinson, R., Aschmann, S.M., Winer, A.M., Carter, W.P.L., 1985. Rate constants for the gas-phase reactions of nitrate radicals with furan, thiophene, and pyrrole at 295 .+-. 1 K and atmospheric pressure. Environ. Sci. Technol. 19, 87–90. https://doi.org/10.1021/es00131a010

Atkinson, R., Aschmann, S.M., Winer, A.M., Pitts, J.N., 1984. Kinetics of the gas-phase reactions of nitrate radicals with a series of dialkenes, cycloalkenes, and monoterpenes at 295 .+-. 1 K. Environ. Sci. Technol. 18, 370–375. https://doi.org/10.1021/es00123a016

Bagot, P., Waring, C., Costen, M., McKendrick, K., 2008. Dynamics of Inelastic Scattering of OH Radicals from Reactive and Inert Liquid Surfaces. J. Phys. Chem. C 112, 10868–10877. https://doi.org/10.1021/jp8024683

Berndt, T., Böge, O., 1997. Gas-phase reaction of NO3 radicals with isoprene: a kinetic and mechanistic study. Int. J. Chem. Kinet. 29, 755–765. https://doi.org/10.1002/(SICI)1097-4601(1997)29:10<755::AID-KIN4>3.0.CO;2-L

Borrás, E., Ródenas, M., Vázquez, M., Vera, T., Muñoz, A., 2015. Particulate and gas-phase products from the atmospheric degradation of chlorpyrifos and chlorpyrifos-oxon. Atmos. Environ. 123, Part A, 112–120. https://doi.org/10.1016/j.atmosenv.2015.10.049

Boyd, C.M., Sanchez, J., Xu, L., Eugene, A.J., Nah, T., Tuet, W.Y., Guzman, M.I., Ng, N.L., 2015. Secondary organic aerosol formation from the β-pinene+NO3 system: effect of humidity and peroxy radical fate. Atmos Chem Phys 15, 7497–7522. https://doi.org/10.5194/acp-15-7497-2015

Canosa-Mas, C.E., Carr, S., King, M.D., Shallcross, D.E., Thompson, K.C., Wayne, R.P., 1999. A kinetic study of the reactions of NO3 with methyl vinyl ketone, methacrolein, acrolein, methyl acrylate and methyl methacrylate. Phys. Chem. Chem. Phys. 1, 4195–4202. https://doi.org/10.1039/A904613E

Carvalho, F.P., 2017. Pesticides, environment, and food safety. Food Energy Secur. 6, 48–60. https://doi.org/10.1002/fes3.108

Chen, Z., Fang, J., Fan, C., Shang, C., 2016. Oxidative degradation of N-Nitrosopyrrolidine by the ozone/UV process: Kinetics and pathways. Chemosphere 150, 731–739. https://doi.org/10.1016/j.chemosphere.2015.12.046

549 Cheng, S., Sun, S., Zhang, H., 2017. Theoretical study on the reaction mechanism of carbaryl
550 with NO3 radical. Theor. Chem. Acc. 136, 60. https://doi.org/10.1007/s00214-017-
551 2093-z
552 Crowley, J.N., Schuster, G., Pouvesle, N., Parchatka, U., Fischer, H., Bonn, B., Bingemer, H.,
553 Lelieveld, J., 2010. Nocturnal nitrogen oxides at a rural mountain-site in south-western
554 Germany. Atmos Chem Phys 18.
555 Davis, D., Pcusazcyk, J., Dwyer, M., Kim, P., 1974. A Stop-Flow Time-of-Flight Mass
556 Spectrometry Kinetics Study. Reaction of Ozone with Nitrogen Dioxide and Sulfur
557 Dioxide. J. Phys. Chem. volume 78, number 18.
558 Derbel, N., Ferchichi, O., Alijah, A., 2018. Tropospheric Reactions of Triazoles with
559 Hydroxyl Radicals: Hydroxyl Addition is Faster than Hydrogen Abstraction.
560 ChemPhysChem 19, 1789–1796. https://doi.org/10.1002/cphc.201800049
561 Désert, M., Ravier, S., Gille, G., Quinapallo, A., Armengaud, A., Pochet, G., Savelli, J.-L.,
562 Wortham, H., Quivet, E., 2018. Spatial and temporal distribution of current-use
563 pesticides in ambient air of Provence-Alpes-Côte-d'Azur Region and Corsica, France.
564 Atmos. Environ. 192, 241–256. https://doi.org/10.1016/j.atmosenv.2018.08.054
565 Dlugokencky, E.J., Howard, C.J., 1989. Studies of nitrate radical reactions with some
566 atmospheric organic compounds at low pressures. J. Phys. Chem. 93, 1091–1096.
567 https://doi.org/10.1021/j100340a015
568 Docherty, K.S., Ziemann, P.J., 2006. Reaction of Oleic Acid Particles with NO_3 Radicals:
569 Products, Mechanism, and Implications for Radical-Initiated Organic Aerosol
570 Oxidation. J. Phys. Chem. A 110, 3567–3577. https://doi.org/10.1021/jp0582383
571 Doussin, J.F., 2003. Etudes cinetiques et mecanistiques des processus d'oxydation des
572 composes organiques volatils d'importance atmospherique induits par le radical nitrate
573 en atmospheres simulees. Paris 7.
574 El Masri, A., Laversin, H., Chakir, A., Roth, E., 2016. Influence of the coating level on the
575 heterogeneous ozonolysis kinetics and product yields of chlorpyrifos ethyl adsorbed
576 on sand particles. Chemosphere 165, 304–310.
577 https://doi.org/10.1016/j.chemosphere.2016.09.036
578 Enami, S., Hoffmann, M., Colussi, A., 2014. In Situ Mass Spectrometric Detection of
579 Interfacial Intermediates in the Oxidation of RCOOH(aq) by Gas-Phase OH-Radicals.
580 J. Phys. Chem. A 118, 4130–4137. https://doi.org/10.1021/jp503387e
581 Finlayson-Pitts, B.J., Pitts, J.N., 2009. Chemistry of the upper and lower atmosphere: theory,
582 experiments, and applications, Nachdr. ed. Academic Press, San Diego, Calif.
583 George, I.J., Abbatt, J.P.D., 2010. Heterogeneous oxidation of atmospheric aerosol particles
584 by gas-phase radicals. Nat. Chem. 2, 713–722. https://doi.org/10.1038/nchem.806
585 Geyer, A., Ackermann, R., Dubois, R., Lohrmann, B., Müller, T., Platt, U., 2001. Long-term
586 observation of nitrate radicals in the continental boundary layer near Berlin. Atmos.
587 Environ. 35, 3619–3631. https://doi.org/10.1016/S1352-2310(00)00549-5
588 Gligorovski, S., Strekowski, R., Barbati, S., Vione, D., 2015. Environmental Implications of
589 Hydroxyl Radicals (•OH). Chem. Rev. https://doi.org/10.1021/cr500310b
590 Goodman, M.A., Aschmann, S.M., Atkinson, R., Winer, A.M., 1988. Kinetics of the
591 atmospherically important gas-phase reactions of a series of trimethyl
592 phosphorothioates. Arch. Environ. Contam. Toxicol. 17, 281–288.
593 https://doi.org/10.1007/BF01055164
594 Graham, R.A., Johnston, H.S., 1974. Kinetics of the gas-phase reaction between ozone and
595 nitrogen dioxide. J. Chem. Phys. 60, 4628–4629. https://doi.org/10.1063/1.1680953
596 Gross, S., Iannone, R., Xiao, S., K. Bertram, A., 2009. Reactive uptake studies of NO 3 and N
597 2 O 5 on alkenoic acid, alkanoate, and polyalcohol substrates to probe nighttime

aerosol chemistry. Phys. Chem. Chem. Phys. 11, 7792–7803. https://doi.org/10.1039/B904741G

Huie, R.E., Herron, J.T., 1974. The rate constant for the reaction O3 + NO2 → O2 + NO3 over the temperature range 259–362 °K. Chem. Phys. Lett. 27, 411–414. https://doi.org/10.1016/0009-2614(74)90253-X

Inserm, 2013. Pesticides : Effets sur la santé - Une expertise collective de l'Inserm.

Kaiser, J.C., Riemer, N., Knopf, D.A., 2011. Detailed heterogeneous oxidation of soot surfaces in a particle-resolved aerosol model. Atmos Chem Phys 11, 4505–4520. https://doi.org/10.5194/acp-11-4505-2011

Karagulian, F., J. Rossi, M., 2005. The heterogeneous chemical kinetics of NO 3 on atmospheric mineral dust surrogates. Phys. Chem. Chem. Phys. 7, 3150–3162. https://doi.org/10.1039/B506750M

Karl, M., Brauers, T., Dorn, H.-P., Holland, F., Komenda, M., Poppe, D., Rohrer, F., Rupp, L., Schaub, A., Wahner, A., 2004. Kinetic Study of the OH-isoprene and O3-isoprene reaction in the atmosphere simulation chamber, SAPHIR. Geophys. Res. Lett. 31, L05117. https://doi.org/10.1029/2003GL019189

Khairy, M.A., Luek, J.L., Dickhut, R., Lohmann, R., 2016. Levels, sources and chemical fate of persistent organic pollutants in the atmosphere and snow along the western Antarctic Peninsula. Environ. Pollut. 216, 304–313. https://doi.org/10.1016/j.envpol.2016.05.092

Khan, M.A.H., Ashfold, M.J., Nickless, G., Martin, D., Watson, L.A., Hamer, P.D., Wayne, R.P., Canosa-Mas, C.E., Shallcross, D.E., 2008. Night-time NO_3 and OH radical concentrations in the United Kingdom inferred from hydrocarbon measurements. Atmospheric Sci. Lett. 9, 140–146. https://doi.org/10.1002/asl.175

Knopf, D., M. Forrester, S., H. Slade, J., 2011. Heterogeneous oxidation kinetics of organic biomass burning aerosol surrogates by O 3 , NO 2 , N 2 O 5 , and NO 3. Phys. Chem. Chem. Phys. 13, 21050–21062. https://doi.org/10.1039/C1CP22478F

Kwok, E.S.C., Atkinson, R., Arey, J., 1995. Observation of Hydroxycarbonyls from the OH Radical-Initiated Reaction of Isoprene. Environ. Sci. Technol. 29, 2467–2469. https://doi.org/10.1021/es00009a046

Lauraguais, A., El Zein, A., Coeur, C., Obeid, E., Cassez, A., Rayez, M.-T., Rayez, J.-C., 2016. Kinetic Study of the Gas-Phase Reactions of Nitrate Radicals with Methoxyphenol Compounds: Experimental and Theoretical Approaches. J. Phys. Chem. A 120, 2691–2699. https://doi.org/10.1021/acs.jpca.6b02729

Li, N., Zhang, P., Yang, B., Shu, J., Wang, Y., Sun, W., 2014. Heterogeneous reaction of particulate chlorpyrifos with NO3 radicals: Products, pathways, and kinetics. Chem. Phys. Lett. 610–611, 70–75. https://doi.org/10.1016/j.cplett.2014.06.062

Liu, C., Gan, J., Zhang, Y., Liang, M., Shu, X., Shu, J., Yang, B., 2011. Heterogeneous Reaction of Suspended Phosmet Particles with NO3 Radicals. J. Phys. Chem. A 115, 10744–10748. https://doi.org/10.1021/jp205175p

Liu, C., Li, S., Gao, R., Dang, J., Wang, W., Zhang, Q., 2014. Mechanism and kinetic properties of NO3-initiated atmospheric degradation of DDT. J. Environ. Sci. 26, 601–607. https://doi.org/10.1016/S1001-0742(13)60388-5

Liu, C., Yang, B., Gan, J., Zhang, Y., Liang, M., Shu, X., Shu, J., 2012. Heterogeneous reactions of suspended parathion, malathion, and fenthion particles with NO3 radicals. Chemosphere 87, 470–476. https://doi.org/10.1016/j.chemosphere.2011.12.031

Liu, C., Yang, B., Zeng, C., 2015. Kinetic studies of heterogeneous reactions of particulate phosmet and parathion with NO3 radicals. Chemosphere 119, 1276–1280. https://doi.org/10.1016/j.chemosphere.2014.09.049

Liu, C.-G., Shu, J.-N., Yang, B., Zhang, P., 2014. Products and kinetics of the heterogeneous reaction of particulate ametryn with NO3 radicals. Environ. Sci. Process. Impacts 16, 2686–2691. https://doi.org/10.1039/c4em00352g

Mattei, C., Wortham, H., Quivet, E., 2018. Heterogeneous atmospheric degradation of pesticides by ozone: Influence of relative humidity and particle type. Sci. Total Environ. 625, 1544–1553. https://doi.org/10.1016/j.scitotenv.2018.01.049

Mattei, C., Wortham, H., Quivet, E., 2019a. Heterogeneous degradation of pesticides by OH radicals in the atmosphere: Influence of humidity and particle type on the kinetics. Sci. Total Environ. 664, 1084–1094. https://doi.org/10.1016/j.scitotenv.2019.02.038

Mattei, C., Dupont, J., Wortham, H., Quivet, E., 2019b. Influence of pesticide concentration on their heterogeneous atmospheric degradation by ozone. Chemosphere. 228, 75–82. https://doi.org/10.1016/j.chemosphere.2019.04.082

Meylan, W.M., Howard, P.H., 1993. Computer estimation of the Atmospheric gas-phase reaction rate of organic compounds with hydroxyl radicals and ozone. Chemosphere 26, 2293–2299. https://doi.org/10.1016/0045-6535(93)90355-9

Moise, T., Talukdar, R.K., Frost, G.J., Fox, R.W., Rudich, Y., n.d. Reactive uptake of NO3 by liquid and frozen organics. J. Geophys. Res. Atmospheres 107, AAC 6-1-AAC 6-9. https://doi.org/10.1029/2001JD000334

Nah, T., Sanchez, J., Boyd, C.M., Ng, N.L., 2016. Photochemical Aging of α-pinene and β-pinene Secondary Organic Aerosol formed from Nitrate Radical Oxidation. Environ. Sci. Technol. 50, 222–231. https://doi.org/10.1021/acs.est.5b04594

Ng, N.L., Brown, S.S., Archibald, A.T., Atlas, E., Cohen, R.C., Crowley, J.N., Day, D.A., Donahue, N.M., Fry, J.L., Fuchs, H., Griffin, R.J., Guzman, M.I., Herrmann, H., Hodzic, A., Iinuma, Y., Jimenez, J.L., Kiendler-Scharr, A., Lee, B.H., Luecken, D.J., Mao, J., McLaren, R., Mutzel, A., Osthoff, H.D., Ouyang, B., Picquet-Varrault, B., Platt, U., Pye, H.O.T., Rudich, Y., Schwantes, R.H., Shiraiwa, M., Stutz, J., Thornton, J.A., Tilgner, A., Williams, B.J., Zaveri, R.A., 2017. Nitrate radicals and biogenic volatile organic compounds: oxidation, mechanisms, and organic aerosol. Atmospheric Chem. Phys. 17, 2103–2162. https://doi.org/10.5194/acp-17-2103-2017

Perring, A.E., Wisthaler, A., Graus, M., Wooldridge, P.J., Lockwood, A.L., Mielke, L.H., Shepson, P.B., Hansel, A., Cohen, R.C., 2009. A product study of the isoprene+NO3 reaction. Atmos Chem Phys 9, 4945–4956. https://doi.org/10.5194/acp-9-4945-2009

Platt, U., LeBras, G., Poulet, G., Burrows, J.P., Moortgat, G., 1990. Peroxy radicals from night-time reaction of N03 with organic compounds. Nature 348, 147–149. https://doi.org/10.1038/348147a0

Platt, U.F., Winer, A.M., Biermann, H.W., Atkinson, R., Pitts, J.N., 1984. Measurement of nitrate radical concentrations in continental air. Environ. Sci. Technol. 18, 365–369. https://doi.org/10.1021/es00123a015

Pöschl, U., Letzel, T., Schauer, C., Niessner, R., 2001. Interaction of Ozone and Water Vapor with Spark Discharge Soot Aerosol Particles Coated with Benzo[a]pyrene: O3 and H2O Adsorption, Benzo[a]pyrene Degradation, and Atmospheric Implications. J. Phys. Chem. A 105, 4029–4041. https://doi.org/10.1021/jp004137n

Salisbury, G., 2001. Production of peroxy radicals at night via reactions of ozone and the nitrate radical in the marine boundary layer. J. Geophys. Res. Atmospheres 106, 12669–12687. https://doi.org/10.1029/2000JD900754

Sauret, N., Wortham, H., Putaud, J.-P., Mirabel, P., 2008. Study of the effects of environmental parameters on the gas/particle partitioning of current-use pesticides in urban air. Atmos. Environ. 42, 544–553. https://doi.org/10.1016/j.atmosenv.2007.09.012

Shiraiwa, M., Garland, R.M., Pöschl, U., 2009. Kinetic double-layer model of aerosol surface chemistry and gas-particle interactions (K2-SURF): Degradation of polycyclic aromatic hydrocarbons exposed to O3, NO2, H2O, OH and NO3. Atmos Chem Phys 9, 9571–9586. https://doi.org/10.5194/acp-9-9571-2009

Sinfort, C., Cotteux, E., Bonicelli, B., Ruelle, B., Douchin, M., Berenger, M., Lagrevol, J., Liet, O., Rudnicki, V.D., 2009. Influence des conditions et matériels de pulvérisation sur les pertes de pesticides au sol et dans l'air en viticulture Languedocienne. Presented at the Colloque National du Groupe Français d'études et d'applications des pesticides, p. 4 p.

Socorro, J., Durand, A., Temime-Roussel, B., Gligorovski, S., Wortham, H., Quivet, E., 2016. The persistence of pesticides in atmospheric particulate phase: An emerging air quality issue. Sci. Rep. 6. https://doi.org/10.1038/srep33456

Socorro, J., Gligorovski, S., Wortham, H., Quivet, E., 2015. Heterogeneous reactions of ozone with commonly used pesticides adsorbed on silica particles. Atmos. Environ. 100, 66–73. https://doi.org/10.1016/j.atmosenv.2014.10.044

Stabel, J.R., Johnson, M.S., Langer, S., 2005. Rate coefficients for the gas-phase reaction of isoprene with NO3 and NO2. Int. J. Chem. Kinet. 37, 57–65. https://doi.org/10.1002/kin.20050

Stutz, J., Wong, K.W., Lawrence, L., Ziemba, L., Flynn, J.H., Rappenglück, B., Lefer, B., 2010. Nocturnal NO3 radical chemistry in Houston, TX. Atmos. Environ. 44, 4099–4106. https://doi.org/10.1016/j.atmosenv.2009.03.004

Suh, I., Lei, W., Zhang, R., 2001. Experimental and Theoretical Studies of Isoprene Reaction with NO3. J. Phys. Chem. A 105, 6471–6478. https://doi.org/10.1021/jp0105950

UIPP, 2017. Repères UIPP 2017/2018 [WWW Document]. URL http://www.uipp.org/flipbook/ (accessed 6.8.18).

Vlasenko, A., George, I.J., Abbatt, J.P.D., 2008. Formation of Volatile Organic Compounds in the Heterogeneous Oxidation of Condensed-Phase Organic Films by Gas-Phase OH. J. Phys. Chem. A 112, 1552–1560. https://doi.org/10.1021/jp0772979

Wang, Y., Yang, B., Zhang, P., Zhang, W., Liu, C., Shu, X., Shu, J., 2012. Heterogeneous Reactions of Pirimiphos-Methyl and Pirimicarb with NO3 Radicals. J. Phys. Chem. A 116, 10802–10809. https://doi.org/10.1021/jp3071635

Wang, Y., Zhang, P., Yang, B., Liu, C., Shu, J., 2013. Kinetic and product study of the heterogeneous reactions of NO3 radicals with suspended resmethrin, phenothrin, and fenvalerate particles. Chemosphere 90, 848–855. https://doi.org/10.1016/j.chemosphere.2012.09.096

Wayne, R.P., Barnes, I., Biggs, P., Burrows, J.P., Canosa-Mas, C.E., Hjorth, J., Le Bras, G., Moortgat, G.K., Perner, D., Poulet, G., Restelli, G., Sidebottom, H., 1991. The nitrate radical: Physics, chemistry, and the atmosphere. Atmospheric Environ. Part Gen. Top., The nitrate radical: Physics, Chemistry, and the Atmosphere 25, 1–203. https://doi.org/10.1016/0960-1686(91)90192-A

Wille, U., Becker, E., Schindler, R.N., Lancar, I.T., Poulet, G., Bras, G.L., 1991. A discharge flow mass-spectrometric study of the reaction between the NO<Subscript>3</Subscript> radical and isoprene. J. Atmospheric Chem. 13, 183–193. https://doi.org/10.1007/BF00115972

Yang, B., Meng, J., Zhang, Y., Liu, C., Gan, J., Shu, J., 2011. Experimental studies on the heterogeneous reaction of NO3 radicals with suspended carbaryl particles. Atmos. Environ. 45, 2074–2079. https://doi.org/10.1016/j.atmosenv.2011.01.052

Yates, S.R., Ashworth, D.J., Zheng, W., Zhang, Q., Knuteson, J., van Wessenbeeck, I.J., 2015. Emissions of 1,3-Dichloropropene and Chloropicrin after Soil Fumigation under

Field Conditions. J. Agric. Food Chem. 63, 5354–5363. https://doi.org/10.1021/acs.jafc.5b01309

Zhang, H., Yang, B., Wang, Y., Shu, J., Zhang, P., Ma, P., Li, Z., 2016. Gas-Phase Reactions of Methoxyphenols with NO3 Radicals: Kinetics, Products, and Mechanisms. J. Phys. Chem. A 120, 1213–1221. https://doi.org/10.1021/acs.jpca.5b10406

Zhao, Z., Husainy, S., Smith, G.D., 2011. Kinetics Studies of the Gas-Phase Reactions of NO3 Radicals with Series of 1-Alkenes, Dienes, Cycloalkenes, Alkenols, and Alkenals. J. Phys. Chem. A 115, 12161–12172. https://doi.org/10.1021/jp206899w

Zivan, O., Bohbot-Raviv, Y., Dubowski, Y., 2017. Primary and secondary pesticide drift profiles from a peach orchard. Chemosphere 177, 303–310. https://doi.org/10.1016/j.chemosphere.2017.03.014

Zivan, O., Segal-Rosenheimer, M., Dubowski, Y., 2016. Airborne organophosphate pesticides drift in Mediterranean climate: The importance of secondary drift. Atmos. Environ. 127, 155–162. https://doi.org/10.1016/j.atmosenv.2015.12.003

761 **SUPPORTING INFORMATION**

762 **Pesticides under study**

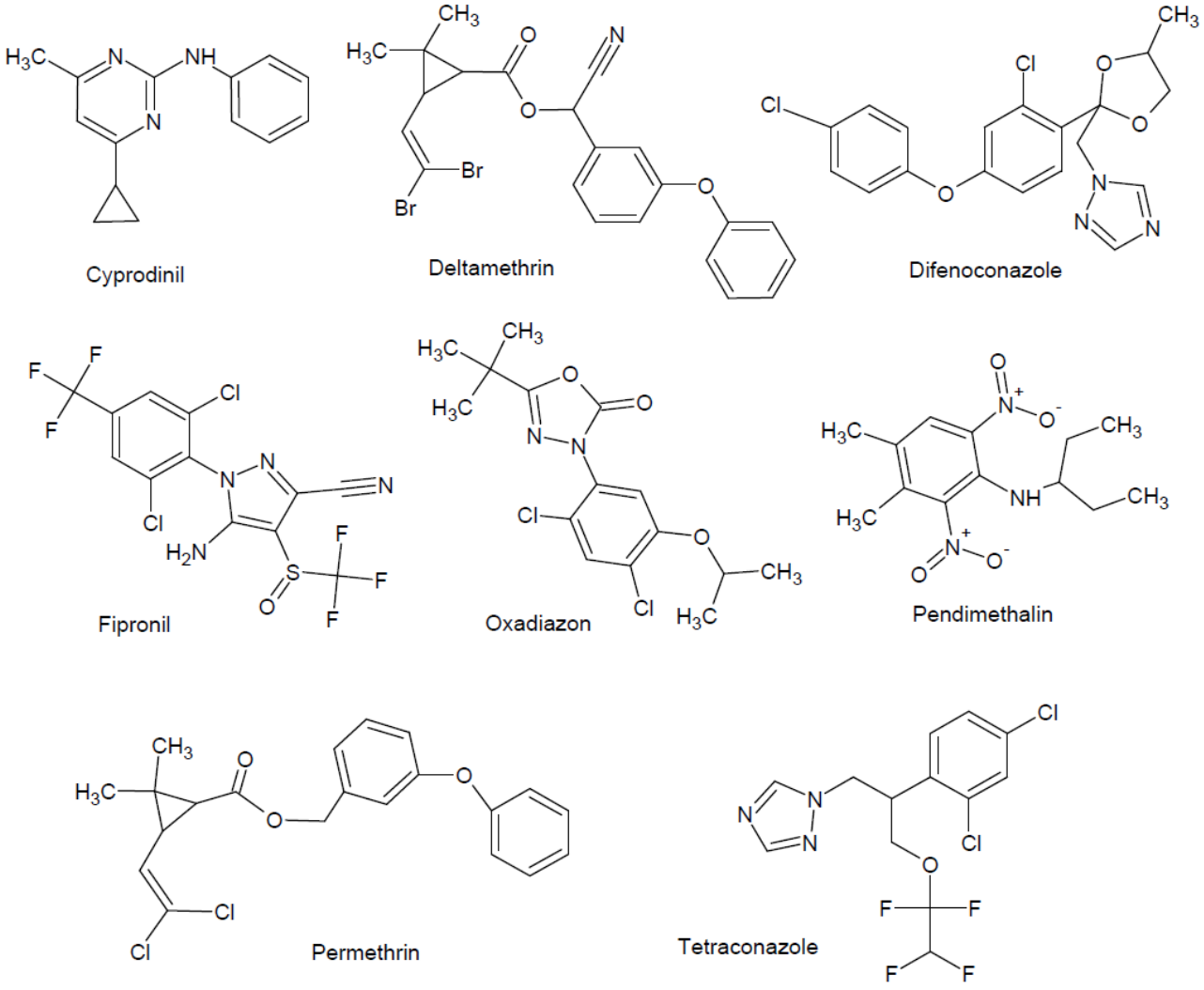

763
764

765

766 Figure S1: Chemical structures of the 8 pesticides under study

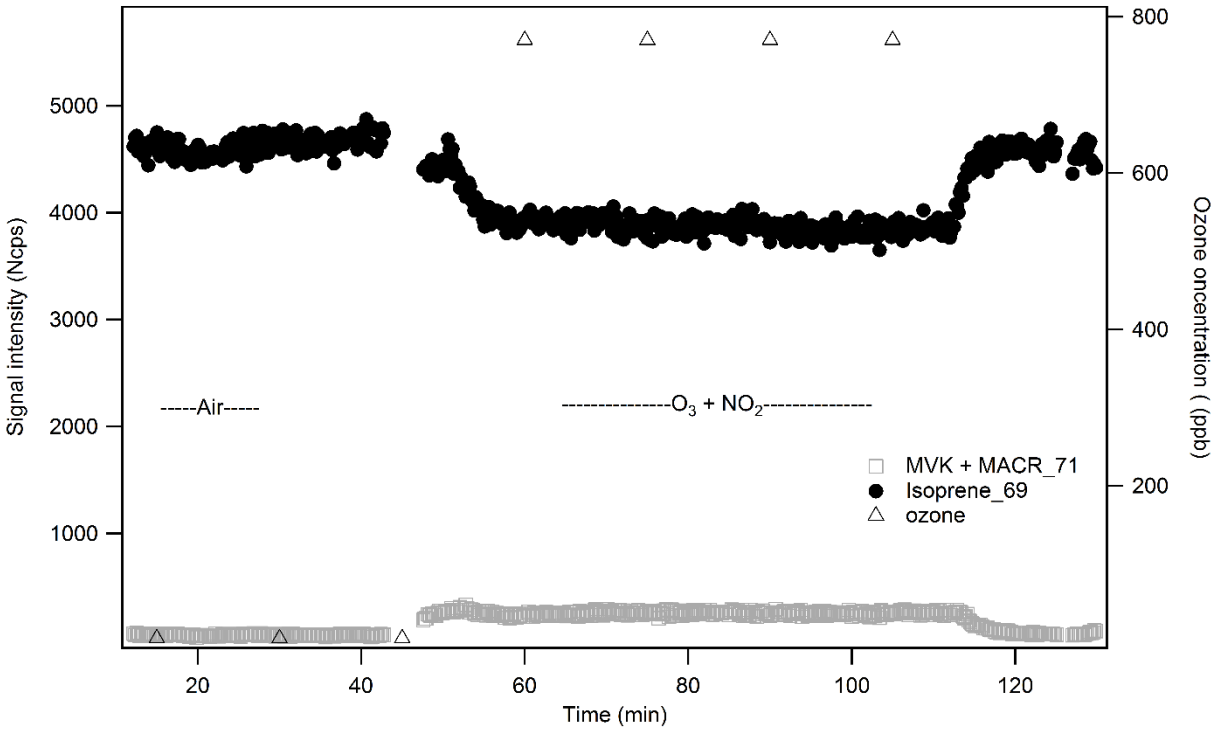

767

768 Figure S2: PTR-MS signal intensity for isoprene (*m/z=69*) and its main degradation product

769 (*m/z=71*) under different oxidation conditions, at 43% RH

770

Table S1: The physicochemical properties of the pesticides

Compounds	Cyprodinil	Deltamethrin	Difenoconazole	Fipronil	Oxadiazon	Pendimethalin	Permethrin	Tetraconazole
CAS number	121552-61-2	52918-63-5	119446-68-3	120068-37-3	19666-30-9	40487-42-1	52645-53-1	112281-77-3
Chemical family	Pyrimidine	Pyrethroïd	Triazole	Pyrazole	Oxadiazole	Dinitroaniline	Pyrethroïd	Triazole
Nature	Fungicide	Insecticide	Fungicide	Insecticide	Herbicide	Herbicide	Insecticide	Fungicide
Molecular weight ($g\ mol^{-1}$)	225.29	505.20	406.26	437.15	345.22	281.31	391.29	372.15
Vapour pressure at 25°C (Pa) [a]	$5.1 \cdot 10^{-4}$	$1.2 \cdot 10^{-8}$	$3.3 \cdot 10^{-8}$	$2.0 \cdot 10^{-6}$	$6.7 \cdot 10^{-4}$	$1.9 \cdot 10^{-3}$	$7.0 \cdot 10^{-6}$	$1.8 \cdot 10^{-4}$
Henry's constant at 25°C ($atm\ m^3\ mol^{-1}$) [b]	$1.91 \cdot 10^{-6}$	$6.06 \cdot 10^{-8}$	$1.69 \cdot 10^{-11}$	$3.17 \cdot 10^{-18}$	$3.22 \cdot 10^{-8}$	$1.45 \cdot 10^{-6}$	$2.88 \cdot 10^{-7}$	$6.20 \cdot 10^{-7}$
Molar volume ($cm^3\ mol^{-1}$) at 20°C and 760 Torr [c]	186.1 ± 3.0	316.7 ± 3.0	287.1 ± 7.0	233.6 ± 7.0	262.4 ± 7.0	231.5 ± 3.0	302.5 ± 3.0	247.1 ± 7.0
Partitioning in particle phase [d]	0.07	0.91	0.99	0.84	0.62	0.01	0.97	0.38
Solubility in water at 20°C ($mg\ L^{-1}$) [a]	13	0.0002	15	3.78	0.57	0.33	0.2	156.6
Characteristic ions	224.05 / 225.10 / 210.03	180.92 / 250.88 / 171.82	322.91 / 324.86	366.87 / 368.84 / 212.87	174.85 / 176.84 / 257.97	252.03 / 161.94	182.98 / 164.84	335.96 / 337.91

[a] PPDB: Pesticide Properties DataBase (sitem.herts.ac.uk/aeru/ppdb)

[b] HENRYWIN™ Software V3.2

[c] SciFinder, calculated using Advanced Chemistry Development (ACD/Labs) Software V11.02 (© 1994-2014 ACD/Labs)

[d] AEROWIN™ Software V1.0 using the Junge-Pankow adsorption mode

Silica particles coating

A uniform particle surface coverage and a coating below a monolayer are assumed to calculate the amount of pesticide adsorbed on the silica particle surface. The particle is considered as a sphere and its radius (r_i, cm) is calculated by eq S1:

$$r_i = \sqrt[3]{\frac{3 \times V_m}{4 \times \pi \times N_A}} \qquad \text{(S1)}$$

where V_m is the molar volume ($cm^3.mol^{-1}$) of pesticide and N_A is the Avogadro number. The molar volume is calculated using Advanced Chemistry Development (ACD/Labs) Software V11.02 (© 1994-2014 ACD/Labs).

S is the surface (cm^2) defined by eq S2 where n is adsorbed pesticide in mole:

$$S = 4 \times \pi \times r_i^2 \times N_A \times n \qquad \text{(S2)}$$

The percentage of the coated aerosol surface T is described by equation S3:

$$T = \frac{S}{S_1} \times 100 \qquad \text{(S3)}$$

where S_1 is the silica particle surface ($m^2\ g^{-1}$).

Table S2: Kinetic constants for the possible reactions in the reactor

Reaction	Kinetic constant (cm^3 $molecules^{-1}$ s^{-1})	Reference
$O_3 + NO_2 \rightarrow NO_3 + O_2$	$(3.50 \pm 0.87) \times 10^{-17}$	Graham et al., 1974, Huie et al., 1974, Davis et al., 1974
NO_3 + isoprene → Products	$(6.5 \pm 0.2) \times 10^{-13}$	Atkinson et al., 1984, Berndt et al., 1997, Stabel et al., 2005, Zhao et al., 2011, Suh et al., 2001, Wille et al., 1991, Dlugokencky et al., 1989
O_3 + isoprene → Products	$(9.6 \pm 0.7) \times 10^{-18}$	Karl et al., 2004
NO_2 + isoprene → Products	$(10.3 \pm 0.3) \times 10^{-20}$	Atkinson, 1984
$NO_3 + O_3 \rightarrow$ Products	$1 \cdot 10^{-17}$	Hjorth et al., 1992
$NO_3 + NO_2 \rightarrow O_2 + NO + NO_2$	$6.56 \cdot 10^{-16}$	DeMore, 1997

Atkinson, R.; Aschmann, S. M.; Winer, A. M.; Pitts, J. N. Kinetics of the Gas-Phase Reactions of Nitrate Radicals with a Series of Dialkenes, Cycloalkenes, and Monoterpenes at 295 .+-. 1 K. *Environ. Sci. Technol.* **1984**, *18* (5), 370–375. https://doi.org/10.1021/es00123a016.

Berndt, T.; Böge, O. Gas-Phase Reaction of NO3 Radicals with Isoprene: A Kinetic and Mechanistic Study. *Int. J. Chem. Kinet.* **1997**, *29* (10), 755–765. https://doi.org/10.1002/(SICI)1097-4601(1997)29:10<755::AID-KIN4>3.0.CO;2-L.

Davis, D.; Pcusazcyk, J.; Dwyer, M.; Kim, P. A Stop-Flow Time-of-Flight Mass Spectrometry Kinetics Study. Reaction of Ozone with Nitrogen Dioxide and Sulfur Dioxide. *The Journal of Physical Chemistry*. 1974, p volume 78, number 18.

DeMore, W. B. Sander. 1997. "Chemical Kinetics and Photochemical Data for Use in Stratospheric Modeling. Evaluation No. 12." https://ntrs.nasa.gov/search.jsp?R=19970037557.

Dlugokencky, E. J.; Howard, C. J. Studies of Nitrate Radical Reactions with Some Atmospheric Organic Compounds at Low Pressures. *J. Phys. Chem.* **1989**, *93* (3), 1091–1096. https://doi.org/10.1021/j100340a015.

Graham, R. A.; Johnston, H. S. Kinetics of the Gas-phase Reaction between Ozone and Nitrogen Dioxide. *J. Chem. Phys.* **1974**, *60* (11), 4628–4629. https://doi.org/10.1063/1.1680953.

Hjorth, J., J. Notholt, and G. Restelli. 1992. "A Spectroscopic Study of the Equilibrium NO2 + NO3 + M 2 N2O5 + M and the Kinetics of the O3/N2O5/NO3/NO2/ Air System." *International Journal of Chemical Kinetics* 24 (1): 51–65. https://doi.org/10.1002/kin.550240107.

Huie, R. E.; Herron, J. T. The Rate Constant for the Reaction O3 + NO2 → O2 + NO3 over the Temperature Range 259–362 °K. *Chem. Phys. Lett.* **1974**, *27* (3), 411–414. https://doi.org/10.1016/0009-2614(74)90253-X.

Karl, M.; Brauers, T.; Dorn, H.-P.; Holland, F.; Komenda, M.; Poppe, D.; Rohrer, F.; Rupp, L.; Schaub, A.; Wahner, A. Kinetic Study of the OH-Isoprene and O3-Isoprene Reaction in the Atmosphere Simulation Chamber, SAPHIR. *Geophys. Res. Lett.* **2004**, *31* (5), L05117. https://doi.org/10.1029/2003GL019189.

Stabel, J. R.; Johnson, M. S.; Langer, S. Rate Coefficients for the Gas-Phase Reaction of Isoprene with NO3 and NO2. *Int. J. Chem. Kinet.* **2005**, *37* (2), 57–65. https://doi.org/10.1002/kin.20050.

Suh, I.; Lei, W.; Zhang, R. Experimental and Theoretical Studies of Isoprene Reaction with NO3. *J. Phys. Chem. A* **2001**, *105* (26), 6471–6478. https://doi.org/10.1021/jp0105950.

Wille, U.; Becker, E.; Schindler, R. N.; Lancar, I. T.; Poulet, G.; Bras, G. L. A Discharge Flow Mass-Spectrometric Study of the Reaction between the NO<Subscript>3</Subscript> Radical and Isoprene. *J. Atmospheric Chem.* **1991**, *13* (2), 183–193. https://doi.org/10.1007/BF00115972.

Zhao, Z.; Husainy, S.; Smith, G. D. Kinetics Studies of the Gas-Phase Reactions of NO3 Radicals with Series of 1-Alkenes, Dienes, Cycloalkenes, Alkenols, and Alkenals. *J. Phys. Chem. A* **2011**, *115* (44), 12161–12172. https://doi.org/10.1021/jp206899w.